Analysis and Optimization of an Electrically Small Receiving Antenna

John P. Casey, *Member, IEEE,* and Rajeev Bansal, *Member, IEEE*

Abstract—**A theoretical and experimental study of an optimum receiving antenna configuration that fits within certain allocated space requirements is presented. The antenna analysis is based on a quasi-static numerical study of a conducting body of revolution above a perfectly conducting ground plane. A general numerical algorithm is developed to determine the input impedance and the effective height of the antenna. In addition, a discussion of the amplifier noise and its role in the choice of the optimum antenna are included. Results are presented for cylindrical and truncated conical structures both with and without a top load.**

I. Introduction

THIS PAPER describes a theoretical and experimental investigation undertaken to optimize an electrically small receiving antenna with the available volume as a constraint. The study includes an analysis of the input impedance and the effective height of the antenna as well as a discussion of the amplifier noise as it pertains to antenna optimization. In particular, the receiving antenna studied in this paper is for Loran-C reception. Fig. 1 is a block diagram of the integrated antenna system, which is designed to be placed on a platform floating on seawater. To be compatible with the navigational receiver, the Loran antenna must be linearly polarized and must provide omni-azimuthal reception at the operational 100-kHz carrier frequency with a 20-kHz bandwidth. The Loran antenna is required to fit within a cylindrical volume that is 4.25 inches in height and 5 inches in diameter.

II. Circuit Analysis

Consider an electrically short monopole of height h above a ground plane as shown in Fig. 2(a). The Thevenin equivalent circuit of the monopole receiving a signal is given in Fig. 2(b), where

- V_{oc} open circuit voltage received by the antenna
- R_a radiation resistance of the antenna
- R_l ohmic resistance of the antenna
- C_a antenna capacitance.

R_l includes the ohmic losses associated with the finite conductivities of the antenna and the seawater ground plane. Since the loss tangent in seawater is very large over the frequency range of concern, the ground plane may be approximated by a perfect conductor. The input impedance of the monopole antenna is $R + 1/j\omega C_a$, where ω is the angular frequency, whereas $R = R_a + R_l$ and $R \ll /j\omega C_a$. The antenna capacitance is obtained by solving an electrostatics problem [1]. In the limiting case of a vanishingly small frequency, a dipole or monopole antenna is just a capacitor. For a uniform incident electric field E^{inc} directed parallel to and in the vicinity of the antenna, the open circuit voltage is given by [2]

$$V_{oc} = E^{inc} h_{eff} \tag{1}$$

where h_{eff} is the effective height of the antenna. The computation of the antenna capacitance and the effective height will be discussed later.

Next, consider the monopole connected by a short wire to the input of an FET amplifier as shown in Fig. 3(a) with equivalent circuit given in Fig. 3(b), where

- C_w interconnection capacitance between the antenna and the amplifier
- R_o input resistance of the amplifier

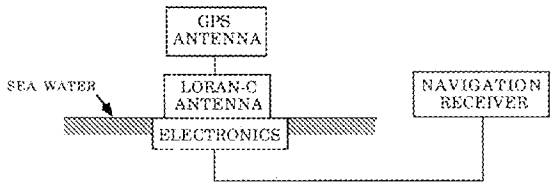

Fig. 1. Loran-C/GPS integrated antenna system.

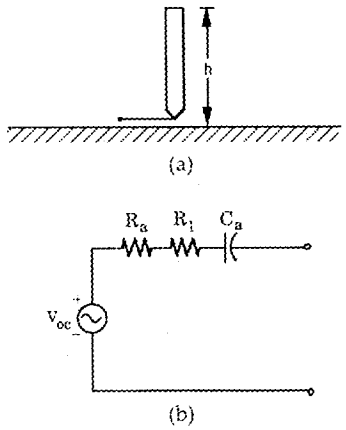

Fig. 2. (a) Monopole antenna above a ground plane; (b) Thevenin equivalent circuit in the receiving mode.

Manuscript received January 22, 1990; revised February 6, 1991.

J. P. Casey is with the Submarine Electromagnetic Systems Department, Naval Underwater Systems Center, New London, CT 06320.

R. Bansal is with the Department of Electrical and Systems Engineering, University of Connecticut, Storrs, CT 06269.

IEEE Log Number 9144862.

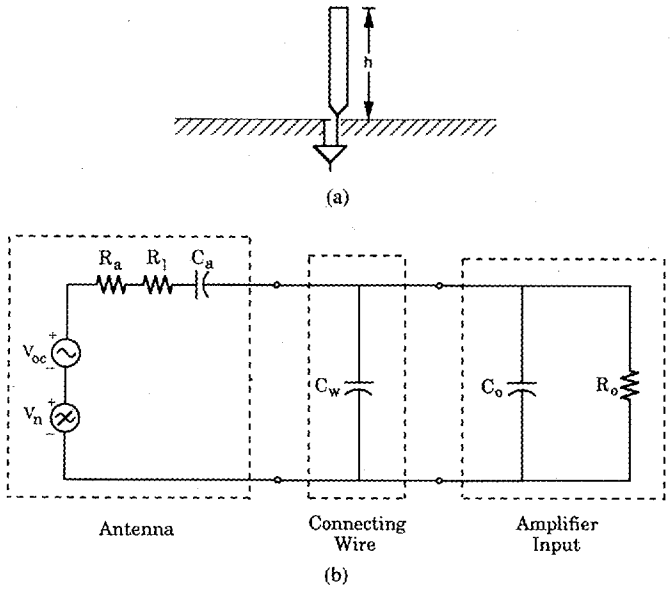

Fig. 3. (a) Monopole antenna connected to an FET amplifier; (b) equivalent circuit.

C_o input capacitance of the amplifier
V_n open circuit noise voltage produced by the amplifier.

To compare the total noise produced by the amplifier with the atmospheric noise received by the antenna, all voltages must be referred to the same location. For convenience, we will refer all noise voltages to the antenna terminals. The thermal noise voltage associated with the loss resistance R_1 of the antenna has been computed to be of negligible value and will not be considered further in this analysis.

To determine the amplifier noise, consider Fig. 4(a) and (b). The voltage E_n and current I_n are equivalent noise sources that adequately represent the noise produced by the amplifier and whose values can easily be determined experimentally [3]. The total noise power produced by the amplifier is given by the sum of the contributions from E_n and I_n. V_{i1} is the voltage produced by E_n at the input terminals of the amplifier, whereas V_{i2} is the voltage produced by I_n at the same location. Y_a, Y_w, and Y_o are the admittances of the antenna, the interconnection, and the amplifier, respectively. An analysis of Fig. 4(a) and (b) yields

$$V_{i1} = E_n\left(\frac{Y_a + Y_w}{Y_a + Y_w + Y_0}\right) \tag{2a}$$

$$V_{i2} = I_n\left(\frac{1}{Y_a + Y_w + Y_0}\right). \tag{2b}$$

V_{i1} and V_{i2} can be referred to equivalent sources at the antenna terminals by considering Fig. 5. In Fig. 5, a voltage source V_s at the antenna terminals produces a voltage V_{is} at the input of the amplifier. An analysis of Fig. 5 yields

$$K_v = \frac{V_{is}}{V_s} = \frac{Y_a}{Y_a + Y_w + Y_0} \tag{3}$$

where K_v is the voltage transfer function. The application of (3) to (2a) and (2b) gives the equivalent amplifier noise

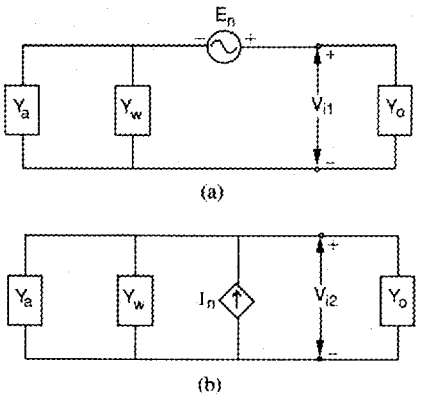

Fig. 4. Amplifier noise model: (a) Input noise voltage E_n of the amplifier; (b) input noise current I_n of the amplifier.

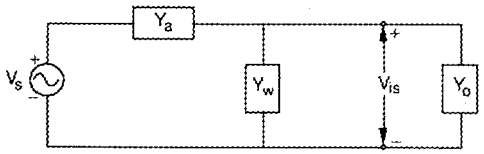

Fig. 5. Equivalent circuit for determination of the voltage transfer function.

voltage sources V_{n1} and V_{n2} due to E_n and I_n, respectively, at the antenna terminals. Therefore, from (2) and (3)

$$V_{n1} = \frac{V_{i1}}{K_v} = E_n\left(1 + \frac{Y_w}{Y_a}\right) \tag{4a}$$

$$V_{n2} = \frac{V_{i2}}{K_v} = I_n\frac{1}{Y_a}. \tag{4b}$$

If V_{n1} and V_{n2} are uncorrelated, the open-circuit noise voltage V_n produced by the amplifier is given by

$$V_n = \left(|V_{n1}|^2 + |V_{n2}|^2\right)^{1/2}$$

$$= \left[|E_n|^2\left|1 + \frac{Y_w}{Y_a}\right|^2 + |I_n|^2\left|\frac{1}{Y_a}\right|^2\right]^{1/2}. \tag{5}$$

Note that V_n is independent of the amplifier impedance.

For convenience, we may relate the amplifier noise voltage to an equivalent incident electric field through the effective height of the receiving antenna. From (1) and (5)

$$E^{amp} = \frac{V_n}{h_{eff}} = \frac{1}{h_{eff}}\left[|E_n|^2\left|1 + \frac{Y_w}{Y_a}\right|^2 + |I_n|^2\left|\frac{1}{Y_a}\right|^2\right]^{1/2}. \tag{6}$$

E^{amp} is the incident electric field parallel to the antenna that produces the same noise power as the amplifier. The substitution of $Y_a \cong j\omega C_a$ and $Y_w = j\omega C_w$ into (6) gives

$$E^{amp} \cong \frac{1}{h_{eff}}\left[|E_n|^2\left(1 + \frac{C_w}{C_a}\right)^2 + |I_n|^2\left(\frac{1}{\omega C_a}\right)^2\right]^{1/2}. \tag{7}$$

The goal of this effort is to design an antenna that produces a minimum value of E^{amp}. Therefore, it is desirable to maximize both the antenna capacitance and the effective height. This requirement results in a tradeoff that will be discussed later. It is preferred that the antenna/amplifier system be atmospheric noise limited, i.e., $E^{amp} < E^{atm}$, where E^{atm} is the atmospheric noise field as determined from the CCIR manual [4].

III. Antenna Capacitance

Consider a body of revolution that is formed by rotating a planar curve about the z axis as described in Fig. 6. In Fig. 6, (ρ, ϕ, z) are cylindrical coordinates, and (t, ϕ) form an orthogonal curvilinear coordinate system on the surface S of the body of revolution. The coordinate t is the arc length along the generating curve, and ϕ is the azimuthal angle measured from the x-z plane. The ends of the generating curve may touch the z axis.

If the body of revolution is a conductor charged to a potential V with respect to a ground plane located on the x-y plane, the following integral equation for the unknown surface charge density σ_s results [1]:

$$\frac{1}{4\pi\epsilon_0}\iint \sigma_s(\boldsymbol{r}')\left(\frac{1}{R^+}-\frac{1}{R^-}\right)dS' = V \qquad \boldsymbol{r}\in S \quad (8)$$

where $\boldsymbol{r}$ and $\boldsymbol{r}'$ are position vectors of the observation and source points, respectively, and the integration is over the surface of the body. In (8), R^+ and R^- denote the distances between the observation and source points on the body and its image, respectively. Since the boundary conditions and excitation are axisymmetric, all field quantities are ϕ independent. Therefore, ϕ may be set equal to zero and suppressed. In the coordinate system of the surface of revolution, (8) may be expressed as

$$\frac{1}{4\pi^2\epsilon_0}\int_0^T q(t')\left[\int_0^{\pi}\left(\frac{1}{R^+}-\frac{1}{R^-}\right)d\phi'\right]dt' = V \qquad r\in S \quad (9)$$

where

$$dt' = \left[(d\rho')^2 + (dz')^2\right]^{1/2} \quad (10)$$

$$R^{\pm} = |\boldsymbol{r}\mp\boldsymbol{r}'| = \left[(\rho-\rho')^2 + (z\mp z')^2 + 4\rho\rho'\sin^2\frac{\phi'}{2}\right]^{1/2}. \quad (11)$$

In (9), the surface charge density has been replaced by the linear charge density $q(t)$, whereas T is the total arc length along the generating curve. The unprimed coordinates refer to the observation point, whereas the primed coordinates refer to the source points. Note that ρ and z can be expressed as functions of t, where (ρ, z) and $\rho', z')$ are the cylindrical coordinates of the points t and t', respectively.

Expression (9) is an integral equation for the unknown linear charge density $q(t)$ along the conducting body of revolution. Once $q(t)$ has been determined, the capacitance C of the body with respect to ground can be evaluated as

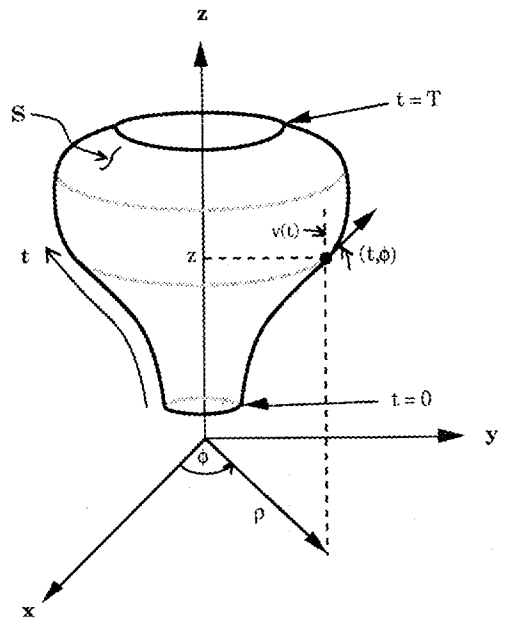

Fig. 6. Body of revolution and coordinate system.

$$C = \frac{Q}{V} = \frac{1}{V}\int_0^T q(t')\,dt'. \quad (12)$$

The method of moments [5] may be applied to obtain a numerical solution to the integral equation (9). In the numerical solution of (9), the generating curve of the body of revolution is approximated as a sequence of N linear segments, as is shown in Fig. 7. An explanation and listing of a FORTRAN language computer program based on the method of moments solution of (9) is given in [6].

Consider a highly conducting tube of length h, radius a, and separated by a distance of s above a perfectly conducting ground plane as illustrated in Fig. 8. Fig. 9 shows a comparison of the computed and measured capacitances of several 6-in-long conducting tubes of different radii plotted as a function of separation above the ground plane. The curves show that the capacitance decreases with separation from the ground plane and increases for larger radii. The data indicate that the measured and computed capacitances agree to within 1 pF for most separations, which is an excellent correspondence considering the margin for error in the measurements. Comparisons for tubes of other heights produced similar results, verifying the accuracy of the body of revolution algorithm.

Reference [7] gives an approximate formula for the capacitance of an electrically small tubular monopole above a perfectly conducting ground plane. This formula is a modified expression for the capacitance of a coplanar stripline. The advantage of this formula over the moment-method solution is that its evaluation involves only the computation of elliptic integrals of the first kind for which simple polynomial approximations exist. Over the range of parameters where the approximate formula is valid, it was found to be in agreement with the integral equation solution and the measured data.

The body of revolution algorithm was also applied to compute the static charge distribution and capacitance of a

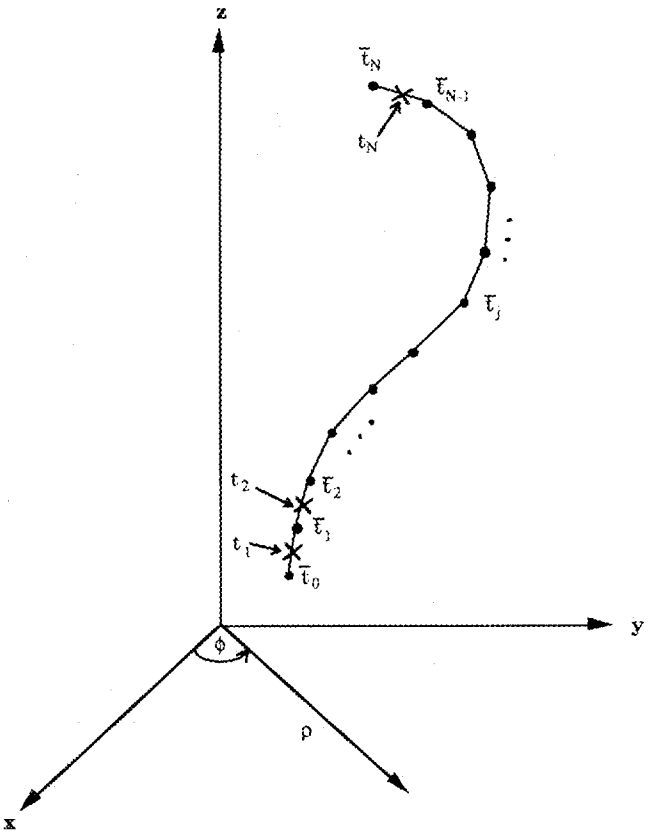

Fig. 7. Approximation of the generating curve as linear segments for the body of revolution in Fig. 6.

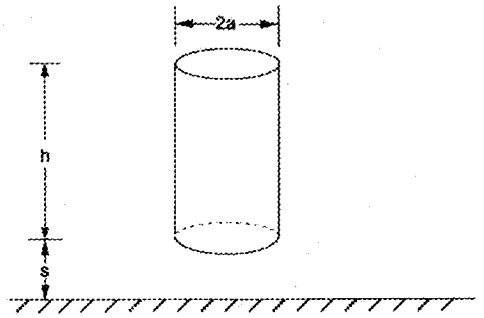

Fig. 8. Conducting tube above a ground plane.

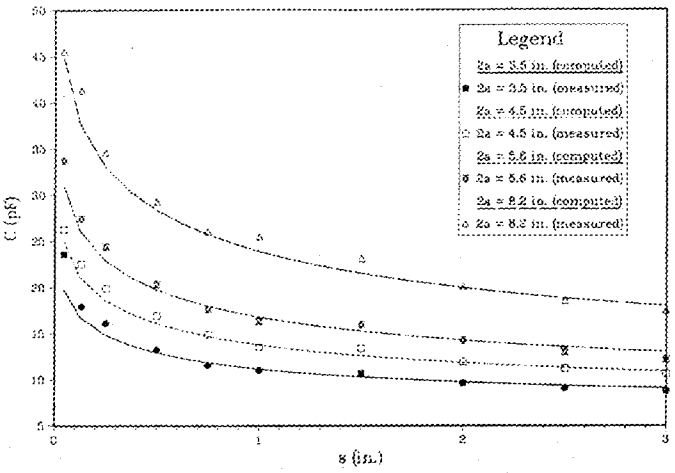

Fig. 9. Capacitances of several conducting tubes ($h = 6$ in) of different radii as a function of separation above a ground plane.

conical antenna over a conducting ground plane. Our computed data compare well with Wilton's computed data [8] for various conical antennas both with and without a top load.

IV. Effective Height

The effective height h_{eff} of a linearly polarized antenna receiving a plane wave from a given direction is the ratio of the magnitude of the open circuit voltage developed at the terminals of the antenna to the magnitude of the electric field strength in the direction of the antenna polarization [9]. This definition has been applied in (1). Alternatively, the effective height is the length of a thin straight conductor oriented perpendicular to the given direction and parallel to the antenna polarization, having a uniform current equal to that at the antenna terminals and producing the same far-field strength as the antenna in that direction [9]. The application of this latter definition to the body of revolution in Fig. 6 yields

$$h_{eff} = \frac{1}{I(0)} \int_0^T I(t) \cos v(t)\, dt \tag{13}$$

where T is the arc length along the generating curve of the antenna, $v(t)$ is the angle between the tangent to the generating curve and the z axis, $I(t)$ is the current along the antenna, and $I(0)$ is the current at the antenna terminals.

An expression for the effective height of a body of revolution may be obtained in terms of the charge distribution. The application of the method-of-moments formulation (Fig. 7) to the effective height formula (13) gives

$$h_{eff} = \frac{1}{I(0)} \sum_{i=1}^{N} \cos v_i \int_{\bar{t}_{i-1}}^{\bar{t}_i} I(t)\, dt. \tag{14}$$

From the use of the continuity equation and the boundary condition $I(T) = 0$, (14) can be expressed as [6]

$$h_{eff} = \frac{\sum_{i=1}^{N} \Delta_i \cos v_i \sum_{j=i}^{N} \gamma_{ij} Q_j \Delta_j}{\sum_{i=1}^{N} Q_i \Delta_i} = \frac{\sum_{i=1}^{N} Q_i \Delta_i (z_i - \bar{z}_0)}{\sum_{i=1}^{N} Q_i \Delta_i} \tag{15}$$

where

$$\gamma_{ij} = \begin{cases} 1/2, & i = j \\ 1, & \text{otherwise.} \end{cases} \tag{16}$$

Q_i is the linear charge density along segment i, whereas Δ_i and z_i are the segment length and the z coordinate of the midpoint of segment i, respectively.

Equation (15) indicates that the effective height of an electrically small body of revolution is actually the axial height of the center of charge. The above expression also shows the importance of capacitive loading at the top of the antenna since it raises the center of charge and thus increases the effective height of the antenna.

Consider the truncated cone described in Fig. 10. It consists of a section of hollow cone with axial length h, lower diameter d_l, and upper diameter d_u. The cone is separated by a small gap s above a perfectly conducting ground plane

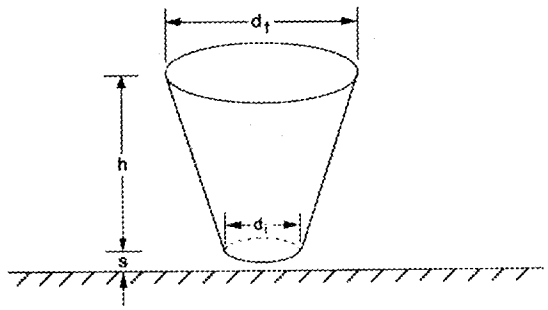

Fig. 10. Truncated cone above a ground plane.

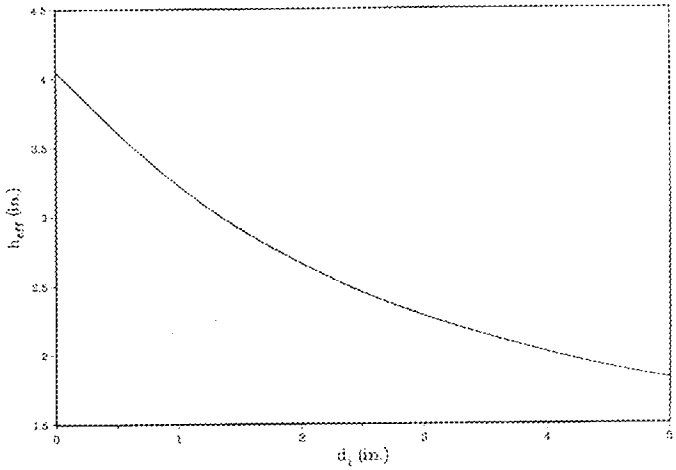

Fig. 11. Effective height of a truncated cone ($h = 6$ in, $d_f = 5$ in) above a ground plane ($s = 0.1$ in) as a function of the lower diameter.

and connected to a receiver below the ground plane by an infinitesimally thin wire. Fig. 11 shows the effective height of a truncated cone with $h = 6$ in, $d_f = 5$ in, and $s = 0.1$ in that is plotted as a function of the lower diameter d_i. A narrower initial diameter reduces the capacitive coupling from the lower end of the cone to ground, thereby raising the center of charge of the antenna. Consequently, the curve shows that the effective height increases with a narrower initial diameter. However, as will be shown in the next section, this increase in effective height is attained at the expense of a decrease in capacitance.

V. Determination of an Optimum Antenna

During this investigation, certain space restrictions for the Loran-C antenna were set. It was decided that the antenna must fit within a 4.25-inch-high, 5-inch-diameter cylinder, where the bottom of the cylinder is coincident with the seawater line. The Loran antenna may be top loaded but must allow for a feed cable to pass through its middle for connection to a GPS antenna. Thus, it was decided to reserve a 0.5-in diameter cylinder in the middle of the Loran antenna for the passage of the GPS antenna feed. The space restrictions for the Loran-C antenna are illustrated in Fig. 12.

Measurements of the FET amplifier were made at 100 kHz to determine the equivalent noise sources E_n and I_n, as defined in Fig. 4. The results of these measurements indicated that for antenna capacitances below 100 pF, the amplifier is current noise limited, i.e., the noise produced due to I_n is much greater than that due to E_n. Therefore, in any

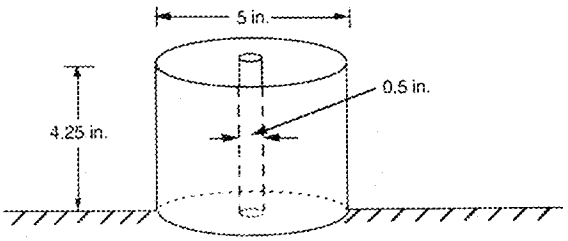

Fig. 12. Space restrictions for the Loran-C antenna.

calculations of the amplifier noise field as determined by (7), the contribution due to E_n will be neglected. The measurements, based on a 100-Hz bandwidth signal with a 100-kHz carrier frequency, indicate that I_n is approximately 2 pA.

In this section, an optimum monopole antenna configuration will be determined. The optimum antenna will be one that fits within the space restrictions as described in Fig. 12 and will result in a minimum amplifier noise field as computed by (7). The antenna geometries to be considered are cylinders and truncated cones. Each structure will be studied both with and without a top load.

A. Cylinder

Consider again the tubular monopole described in Fig. 8 with $h = 4.15$ in and $s = 0.1$ in. The antenna capacitance, effective height, and amplifier noise field are plotted as functions of the tube diameter in Figs. 13(a), (b), and (c), respectively. The curves show that the antenna capacitance is a monotonically increasing function of the tube diameter, whereas the effective height is a decreasing function. The amplifier noise field E^{amp} as computed from (7) is inversely proportional to the product of the effective height and the antenna capacitance for a current noise limited system. Fig. 13(c) shows that E^{amp} is a monotonically decreasing function of the tube diameter. Therefore, the change in capacitance due to a variation in the tube diameter overrides the opposite change in the effective height. For example, a tubular monopole with $2a = 0.5$ in yields $C_a = 3.52$ pf, $h_{eff} = 1.80$ in, and $E^{amp} = 19.8$ μV/m, whereas a tube with $2a = 5$ in gives $C_a = 22.4$ pf, $h_{eff} = 1.32$ in, and $E^{amp} = 4.24$ μV/m. Upon increasing the tube diameter from 0.5 to 5 in, the capacitance increases by more than a factor of 6 and the effective height decreases by less than 1.5. Consequently, the amplifier noise field decreases by more than a factor of 4.5, corresponding to an improvement of 13.4 dB. Thus, the data in Fig. 13(c) indicate that the optimum tubular monopole is one with the maximum allowable diameter ($2a = 5$ in).

If the tube is top loaded with a 0.5-inch-inner diameter, 5-inch-outer diameter conducting annular disk, some improvement in performance can be obtained. For example, a top-loaded tube with $h = 4.15$ in, $s = 0.1$ in, and $2a = 0.5$ in results in $C_a = 7.36$ pf, $h_{eff} = 3.23$ in, and $E^{amp} = 5.27$ μV/m, whereas a tube with $2a = 5$ in gives $C_a = 22.7$ pf, $h_{eff} = 1.39$ in, and $E^{amp} = 3.96$ μV/m. Thus, top loading provides an 11.5-dB decrease in the amplifier noise field for the 0.5-inch-diameter tube while only resulting in a 0.59-dB improvement for the 5.0-inch-diameter tube. However, the larger tube still gives the best performance.

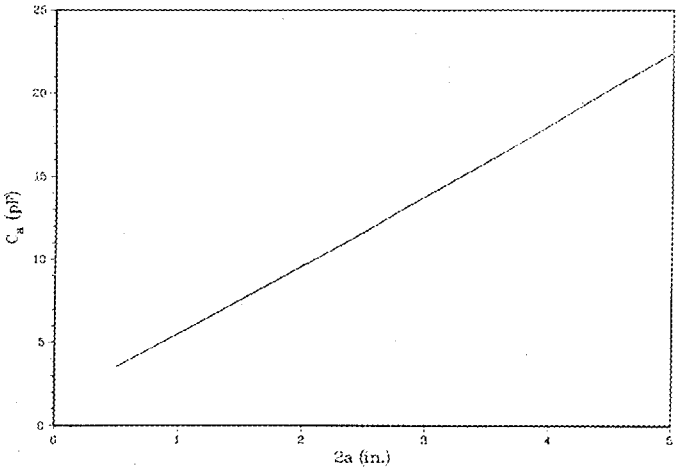

(a)

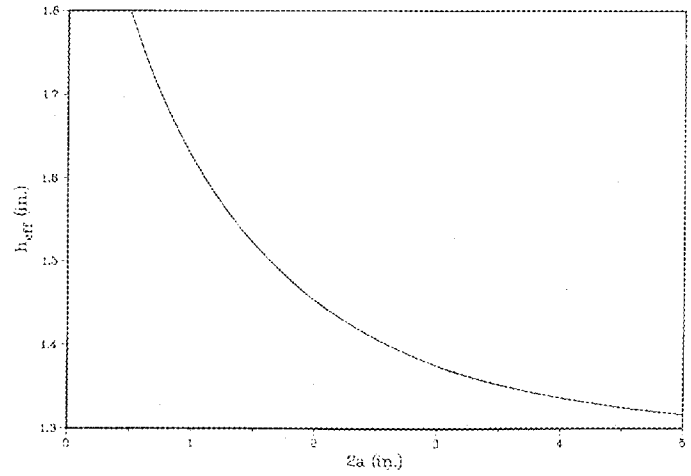

(b)

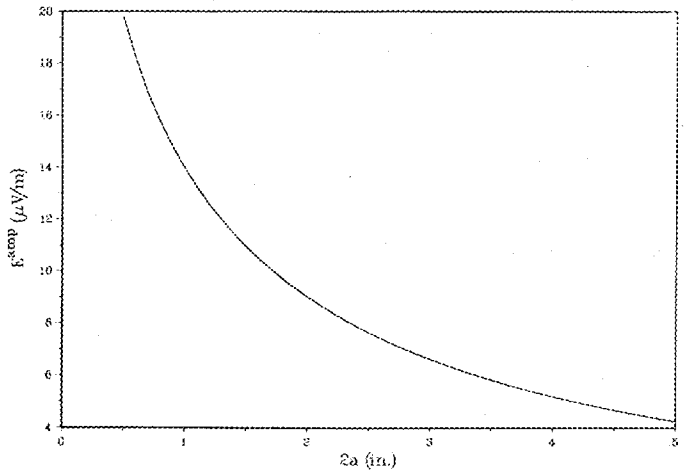

(c)

Fig. 13. (a) Capacitance of a conducting tube ($h = 4.15$ in) above a ground plane ($s = 0.1$ in) as a function of diameter; (b) effective height of a conducting tube ($h = 4.15$ in) above a ground plane ($s = 0.1$ in) as a function of diameter; (c) amplifier noise field due to a current noise limited FET ($I_n = 2$ pA, $f = 100$ kHz) for the conducting tube described in (a) and plotted as a function of the tube diameter.

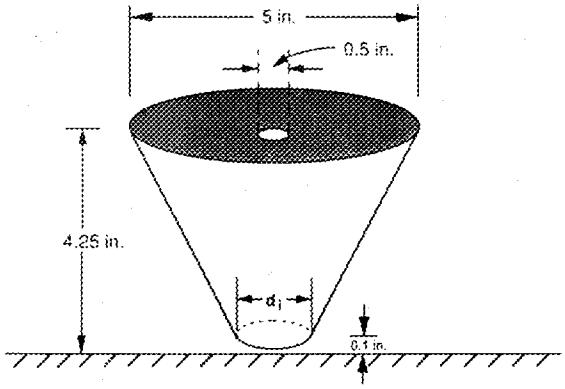

Fig. 14. Top-loaded truncated cone above a ground plane.

B. Truncated Cone

Consider the top-loaded truncated cone described in Fig. 14. The antenna capacitance, effective height, and amplifier noise field are plotted as functions of the lower diameter d_i in Figs. 15(a), (b), and (c), respectively, for the truncated cone both with and without the top load. The curves show that the antenna capacitance increases with d_i, whereas the effective height exhibits the opposite behavior. In addition, Fig. 15(c) indicates that E^{amp} is a monotonically decreasing function of d_i. Consequently, the increase in capacitance associated with an increase in the lower diameter overrides the corresponding decrease in the effective height. Therefore, tapering the antenna at the base does not provide an improvement in the overall antenna performance. For example, an unloaded cone with $d_i = 0.5$ in results in $E^{amp} = 5.02$ μV/m, whereas one with $d_i = 5.0$ in gives $E^{amp} = 4.24$ μV/m. This increase in the lower diameter only results in a 1.47-dB improvement in the amplifier noise field. Note that a truncated cone with $d_i = d_f$ is just a cylinder. The amplifier noise curves in Fig. 15(c) show that the cylindrical monopole with $2a = 5$ in provides a lower amplifier noise field than a truncated cone.

Fig. 15(c) shows that a top-loaded cone provides a lower amplifier noise field than an unloaded cone. However, this improvement is quite small. For example, a top-loaded truncated cone with $d_i = 0.5$ in results in only a 0.67-dB improvement over an unloaded one.

VI. Final Design

The analysis of the previous section has shown that the optimum Loran-C antenna that fits within the space restrictions described in Fig. 12 is a tubular monopole with the maximum allowable diameter ($2a = 5$ in). From Figs. 13(a)–(c), this antenna results in $C_a = 22.4$ pF, $h_{eff} = 1.32$ in, and $E^{amp} = 4.24$ μV/m. Although the analysis showed that a top-loaded tube performs slightly better than an unloaded tube (0.59-dB improvement) the top load was omitted for mechanical reasons.

Fig. 16 gives a schematic view of the Loran-C antenna and amplifier assembly. For mechanical reasons, the antenna and the amplifier were enclosed in a 1/16-inch-thick, 5-inch-outer diameter fiberglas tube. The antenna was constructed from a 1/16-inch-thick aluminum tube that fit tightly against the

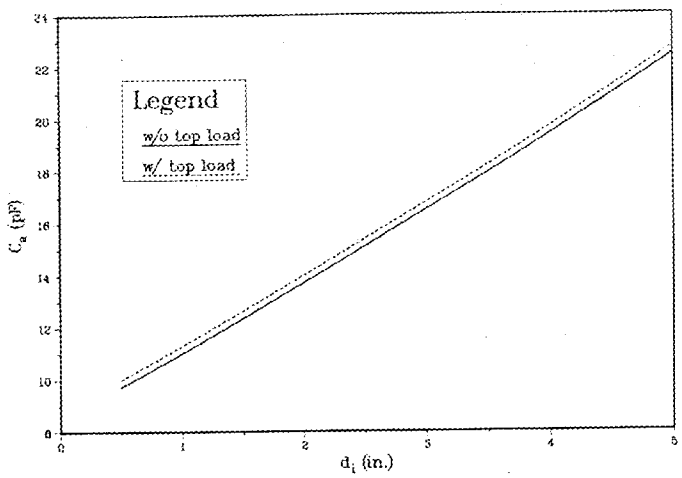

(a)

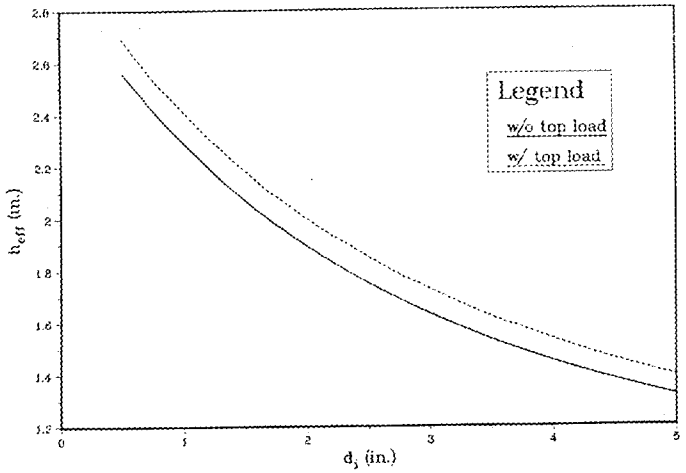

(b)

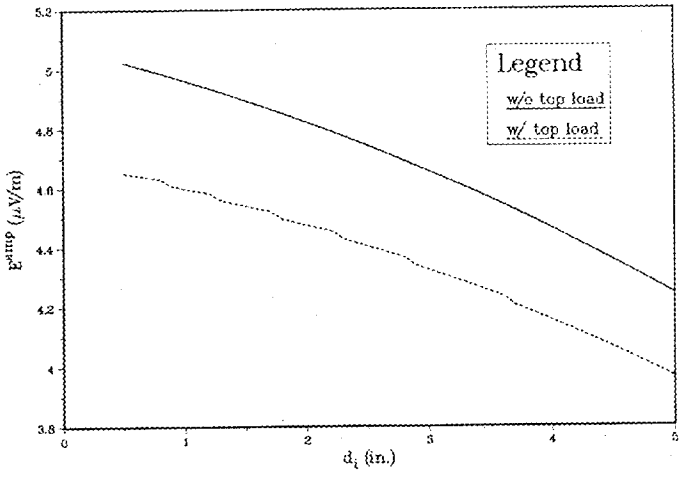

(c)

Fig. 15. (a) Capacitance of the truncated cone described in Fig. 14 as a function of the lower diameter; (b) effective height of the truncated cone described in Fig. 14 as a function of the lower diameter; (c) amplifier noise field due to a current noise limited FET (I_n = 2 pA, f = 100 kHz) for the truncated cone described in Fig. 14 and plotted as a function of the lower diameter.

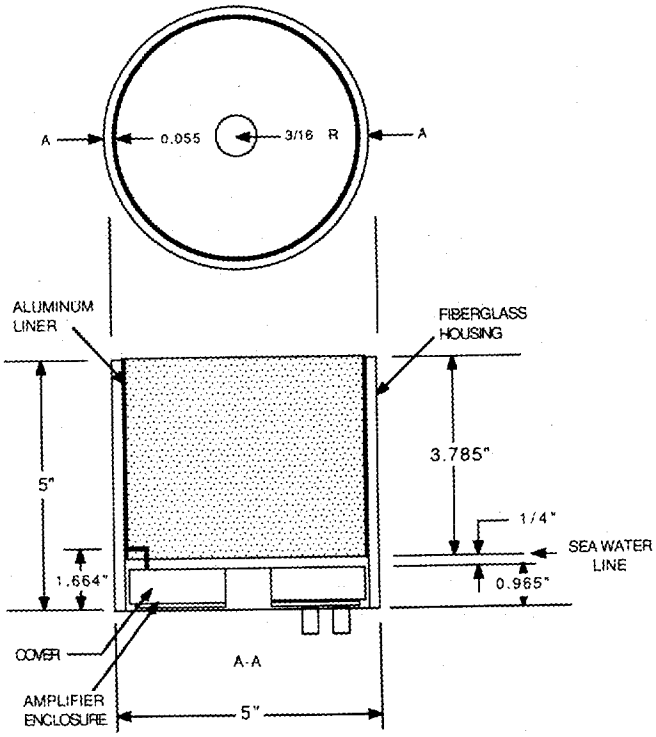

Fig. 16. Schematic view of the Loran-C antenna.

fiberglas housing. The amplifier was enclosed in a 0.965-inch-high grounded aluminum can that was the same diameter as the antenna. The can included a 3/16-inch-diameter hole through its middle for passage of the GPS antenna feed cable. The Loran-C antenna and amplifier assembly in Fig. 16 was enclosed in a cylindrical radome made of lexan ($\epsilon_r \cong 3$) and further surrounded by a floatation collar made of syntactic foam ($\epsilon_r \cong 1.5$).

Since the amplifier required a larger enclosure than previously anticipated (0.965-inch-height instead of 0.75 in), the antenna height was reduced to 3.785 in, whereas the fiberglas housing reduced the antenna diameter to approximately 4-7/8 in. Additionally, the tube was separated by 0.25 in from the ground plane. The recalculation of the parameters for this smaller antenna (h = 3.785 in, $2a$ = 4.875 in, and s = 0.25 in) yields C_a = 17.8 pF h_{eff} = 1.53 in, and E^{amp} = 4.60 μV/m. From the CCIR tables [4], the atmospheric noise (for a 100-Hz bandwidth) near the coast of Connecticut ranges from a minimum of 0.94 μV/m during the winter to a maximum of 21 μV/m during the summer. Thus, according to these numbers, the Loran antenna/amplifier system is usually atmospheric noise limited.

The effective height of the Loran antenna was measured by comparing the received signal strength from a Loran station with that from a VLF loop antenna of known effective height. Based on this method, the measured effective height was approximately 1 in, which is smaller than the number predicted. The smaller measured effective height is probably due to the added capacitive loading from the dielectric surrounding the antenna and the finite thickness of the connecting wire. The measurements were carried out over a saltwater pond on Fisher's Island, NY.

VII. Summary and Conclusions

This paper has provided a systematic theoretical determination of an optimum monopole antenna configuration for Loran-C reception that fits within certain space requirements. The antenna analysis was based on a quasi-static numerical study of a conducting body of revolution above a perfectly conducting ground plane. An optimum antenna is one that results in a minimum amplifier noise field as computed from (7).

An integral part of this study included a determination of the amplifier noise. On account of the small dimensions allotted for the Loran antenna, the antenna capacitance was sufficiently small so that the amplifier was current noise limited (see Fig. 4), resulting in a noise field that is inversely proportional to the product of the antenna capacitance and effective height. Consequently, the study showed a tradeoff in the effort to obtain both a large antenna capacitance and effective height. For example, a structure that is more tapered at the base yields an increase in effective height at the expense of a loss in capacitance. The analysis showed that the optimum monopole antenna is a hollow cylinder of maximum allowable diameter and a small separation from the ground plane. The analysis also indicated that the addition of a top load provides a small increase in both the antenna capacitance and effective height resulting in an improved performance. However, because of mechanical constraints, it was decided to omit the top load.

Measurements performed on the Loran-C antenna indicate a lower effective height than the predicted value because of the finite thickness of the connecting wire and the added shunt capacitive loading from the dielectric surrounding the antenna. The numerical algorithm for the conducting body of revolution assumes an upper-half space consisting of air and does not account for any dielectric loading.

References

[1] S. A. Schelkunoff and H. T. Friis, *Antennas: Theory and Practice*. New York: Wiley, 1952, ch. 10.

[2] E. C. Jordan and K. G. Balmain, *Electromagnetic Waves and Radiating Systems*. Englewood Cliffs, NJ: Prentice-Hall, 1968, pp. 351–353.

[3] C. D. Motchenbacher and F. C. Fitchen, *Low-Noise Electronic Design*. New York: Wiley, 1973.

[4] CCIR Rep. 322, "World distribution and characteristics of atmospheric noise," Int. Telecommunication Union, Geneva, 1964.

[5] R. F. Harrington, *Field Computation by Moment Methods*. Malabar, FL: R. E. Krieger, 1982.

[6] J. P. Casey and R. Bansal, "Analysis and design of a loran-C antenna," NUSC Tech. Rep. 8643, Naval Underwater Syst. Cent., New London, CT, Oct. 18, 1989.

[7] ——, "Capacitance of a small tubular antenna," *Electron. Lett.*, vol. 24, pp. 1021–1022, Aug. 4, 1988.

[8] D. R. Wilton, "Static analysis of conical antenna over a ground plane," Univ. Mississippi, Air Force Office of Scientific Research, Bolling AFB, Washington, DC, Aug. 1976.

[9] IEEE, "IEEE standard definitions of terms for antennas," IEEE Std. 145-1983; *IEEE Trans. Antennas Propagat.*, vol. AP-31, pt. II, Nov. 1983.

John P. Casey (S'83–M'87) was born in Hartford, CT, on November 2, 1952. He received the B.S., M.S., and Ph.D. degrees in electrical engineering from the University of Connecticut, Storrs, in 1978, 1979, and 1987, respectively.

From 1979 to 1980, he was employed by The Johns Hopkins University Applied Physics Laboratory, Laurel, MD, working on the design of waveguides and applying magnetohydrodynamic theory to submarine detection problems. Since 1981, he has been with the Submarine Electromagnetic Systems Department of the Naval Underwater Systems Center, New London, CT, where he is involved with the analysis and design of submarine antenna systems. His research interests include electromagnetic theory, antenna analysis, and numerical techniques.

Dr. Casey is a member of Eta Kappa Nu, Tau Beta Pi, and Phi Kappa Phi.

Rajeev Bansal (S'79–M'81) received the B. Tech degree in electrical engineering from the Indian Institute of Technology, Kanpur, in 1976. He received the S.M. and Ph.D. degrees in applied physics from Harvard University in 1977 and 1981, respectively.

From 1977 through 1981, he was a Research Assistant in the Antenna Group at the Gordon McKay Laboratory of Harvard University. In 1981, he joined the faculty of the University of Connecticut, Storrs, where he is currently an Associate Professor of Electrical and Systems Engineering. His research interests are antenna analysis and applied electromagnetics.

Dr. Bansal is an Associate Editor of the *IEEE Antennas and Propagation Magazine*.